Radiotherapy and Oncology 173 (2022) 93–101

Contents lists available at ScienceDirect

Radiotherapy and Oncology

journal homepage: www.thegreenjournal.com

Original Article

Improving workflow for adaptive proton therapy with predictive anatomical modelling: A proof of concept

Ying Zhang [a,*], Jailan Alshaikhi [b], Richard A. Amos [a], Matthew Lowe [c,d], Wenyong Tan [e], Esther Bär [a,f], Gary Royle [a]

[a] Department of Medical Physics and Biomedical Engineering, University College London, United Kingdom; [b] Saudi Proton Therapy Center, King Fahad Medical City, Riyadh, Saudi Arabia; [c] Christie Medical Physics and Engineering, The Christie NHS Foundation Trust; [d] Division of Cancer Sciences, Faculty of Biology, Medicine and Health, The University of Manchester, Manchester, United Kingdom; [e] Department of Oncology, Shenzhen Hospital of Southern Medical University, China; [f] University College London Hospitals NHS Foundation Trust, United Kingdom

ARTICLE INFO

Article history:
Received 21 December 2021
Received in revised form 29 May 2022
Accepted 31 May 2022
Available online 3 June 2022

Keywords:
Head and neck cancer
Intensity-modulated proton therapy
Application of anatomical modelling

ABSTRACT

Purpose: To demonstrate predictive anatomical modelling for improving the clinical workflow of adaptive intensity-modulated proton therapy (IMPT) for head and neck cancer.

Methods: 10 radiotherapy patients with nasopharyngeal cancer were included in this retrospective study. Each patient had a planning CT, weekly verification CTs during radiotherapy and predicted weekly CTs from our anatomical model. Predicted CTs were used to create predicted adaptive plans in advance with the aim of maintaining clinically acceptable dosimetry. Adaption was triggered when the increase in mean dose (D_{mean}) to the parotid glands exceeded 3 Gy(RBE). We compared the accumulated dose of two adaptive IMPT strategies: 1) Predicted plan adaption: One adaptive plan per patient was optimised on a predicted CT triggered by replan criteria. 2) Standard replan: One adaptive plan was created reactively in response to the triggering weekly CT.

Results: Statistical analysis demonstrates that the accumulated dose differences between two adaptive strategies are not significant ($p > 0.05$) for CTVs and OARs. We observed no meaningful differences in D_{95} between the accumulated dose and the planned dose for the CTVs, with mean differences to the high-risk CTV of −1.20 %, −1.23 % and −1.25 % for no adaption, standard and predicted plan adaption, respectively. The accumulated parotid D_{mean} using predicted plan adaption is within 3 Gy(RBE) of the planned dose and 0.31 Gy(RBE) lower than the standard replan approach on average.

Conclusion: Prediction-based replanning could potentially enable adaptive therapy to be delivered without treatment gaps or sub-optimal fractions, as can occur during a standard replanning strategy, though the benefit of using predicted plan adaption over the standard replan was not shown to be statistically significant with respect to accumulated dose in this study. Nonetheless, a predictive replan approach can offer advantages in improving clinical workflow efficiency.

Intensity modulated proton therapy (IMPT) offers the potential to limit dose to normal tissues for head and neck (H&N) cancer patients [1–5]. However, this precise delivery technique has inherent sensitivity to uncertainties. A major source of uncertainty in the delivery of IMPT to the H&N region, comes from patients not being static during the course of the treatment. Anatomical changes caused by weight loss and/or tumour shrinkage are common and can lead to dosimetric discrepancies [6–8]. Wu *et al.* [8] showed that the mean doses of CTVs were reduced up to 7 % at a week 4 verification scan in a cohort of oropharyngeal patients. Yang *et al.* [9] reported that 40 % of patients with head and neck cancer who undergo IMPT at their institution require plan adaption.

Adaptive proton therapy is key to mitigate the dosimetric discrepancies caused by geometric variations [10,11]. Two adaption strategies are available: online adaption, where the plan is altered in real-time while the patient is in the treatment position, and offline adaption, which is done away from the treatment room and where changes are only applied to subsequent fractions once an adapted plan has been prepared. While optimal for patient treatment, online adaption poses challenges in terms of computational speed and pre-delivery quality assurance (QA) for plan verification [12–15]. Offline adaption is generally used in proton therapy facilities. However, this presents challenges to the clinical workflow

* Corresponding author at: Department of Medical Physics and Biomedical Engineering, University College London, Gower Street, London WC1E 6BT, United Kingdom.
E-mail address: ying.zhang.18@ucl.ac.uk (Y. Zhang).

https://doi.org/10.1016/j.radonc.2022.05.036
0167-8140/

efficiency. While plans are adapted, patients must either continue treatment with an existing sub-optimal plan or face interruptions to treatment. The latter may be particularly undesirable for rapidly growing tumours such as squamous carcinomas of the H&N [16]. Furthermore, a reactive approach to plan adaption can create an unpredictable workload for treatment planning staff, as well as for the medical physics team who perform patient-specific plan QA, and for radiation oncologists who review and approve the plans.

Adaptive plans that can be prepared in advance would be beneficial to the clinical workflow: 1) The adapted replan can be delivered as soon as it is needed due to the ability to perform patient-specific QA/verification before the adaption is required, for example, on a predicted CT, which triggered a replan. 2) For the patient, there is no gap in treatment or the delivery of a few sub-optimal fractions while the replan is calculated, approved, and verified through QA. 3) For the workflow, the option to prepare adaptive plans in advance allows for easier scheduling of patient-specific QA around machine QA, maintenance, and other demands for beam time.

We investigated the use of a predictive anatomical model to generate adaptive proton therapy plans in advance of their requirement. We aim to show a proof of concept of a prospective offline adaptive technique for creating predicted adapted plans in advance, benchmarked against a standard reactive clinical replanning technique. Twenty nasopharyngeal carcinoma (NPC) patients who had previously received photon radiotherapy and had a planning CT and weekly CTs during the course of treatment were used to build and verify a predictive anatomical model.

Materials and methods

A. Predictive anatomical model

Details of the mathematical formalism of the anatomical models alongside a validation of the models' predictive power are given in Zhang *et al.* [17], and summarised here. To build the model, we randomly selected a patient from the cohort and applied a leave-one-out cross-validation strategy to obtain the average deformation of our training population (n = 19) per week (average model). To predict a deformation for the remaining patient, the average deformation of the training population was applied to the patient's planning CT. The model was then updated based on the patient's progression during treatment (predictive anatomical model). This process is repeated for 10 randomly selected patients. It follows that each validation patient is independent from the training population used to create the average model.

The predictive ability of our model has been validated based on CT numbers, contours, proton spot location deviations and dose distribution in [17]. Compared with no model, in which predicted images were replaced by planning CT, the predictive model reduced the average CT number difference between predicted CTs and real CTs at week 3 by 18.8 HU with approximately 2 million voxels analysed. The average gamma index (using 2 mm/2%) between the dose calculated on predicted CT and real CT at week 3 was improved from 96.1 % (94.4 %-97.8 %) for no model to 97.1 % (95.8 %-98.3 %) for the predictive model.

B. Patient data

Ten validation patients were included in this study. Each patient has a planning CT (pCT), weekly verification CTs and predicted weekly CTs. Contours in the planning CT and weekly CTs were manually delineated by an oncologist. None of the IMPT plans presented in this study were applied during the clinical radiotherapy treatment of these patients. Instead, this is a retrospective study using the patients' imaging data. As tumour location and size are diverse in this dataset, predicting the change to the high-risk CTV (tumour) is challenging. The model is most effective in predicting the patient outline and parotid gland positions. Hence, for all OAR contours and the low-risk CTV (nodal area) affected by neck changes, we used the predicted contours from contour propagation. For the high-risk CTV, we used the initial CTV of the planning CT in the predicted plan to ensure target coverage. In this study, plan adaption was triggered with the aim of protecting the parotid glands, following the TORPEdO trial (A phase III trial of proton therapy versus intensity-modulated radiotherapy for multitoxicity reduction in oropharyngeal cancer; CRUK/18/010) [18]. When the difference in D_{mean} (between the original plan calculated on the planning CT and a weekly verification CT) to both parotid glands was larger than 3 Gy(RBE) [19], we instigated a replan. Detailed clinical information of this cohort of patients can be found in [20].

For all 10 validation patients, an original (nominal) IMPT treatment plan with five fields (60°, 110°, 180°, 250°, 300°) was generated using Eclipse version 16.1.0 (Varian Medical Systems, Palo Alto, CA). All plans generated throughout this study were robustly optimized with ± 3 mm setup and ± 3.5 % range uncertainty for CTVs and critical organs at risk (OARs). A relative biological effectiveness (RBE) of 1.1 for proton beams was used. The dosimetric goals and priorities for all plans in this study are summarised in Table 1 [4,21–23]. Further details can be found in Appendix A.

The nominal plan was recalculated on the weekly verification CTs and evaluated to identify the need for adaption. Adaption was required for 9 out of 10 patients (exception: patient ID 1 referred to in later tables), and adapted plans were generated using the CTs that triggered the replan.

A plan was deemed acceptable if the goals set for the CTV and serial organs were fulfilled in the nominal scenario (the error-free distribution) as well as all 12 dose distributions (3 mm orthogonal shifts combined with the ± 3.5 % range error) in a robust evaluation. Rigid registration provided by Niftyreg[1] was used before plan recalculation. For dose distributions calculated on weekly CT images, the DIR algorithm of Niftyreg [24] was used to accumulate the dose in the reference frame of the planning CT.

C. Adaptive planning using the predictive anatomical model

An adaptive strategy that uses the predicted images to create an adapted proton plan in advance of its necessity was proposed and compared with the standard replan approach in which the replan is produced in response to an identified clinical need.

1. Predicted plan adaption.

The predicted plan adaption strategy comprised of one plan adaption. For that strategy, the nominal treatment plan was recalculated on each of the weekly predicted images and the resulting dose distribution was assessed. The prospective replan was created in the predicted image where the recalculated dose distribution met the conditions required to trigger plan adaption. The adapted plan was then applied as soon as the verification CT collected during treatment triggered replan. Note that during this strategy, the adapted plan is not necessarily applied in the week that predicted adaption, but rather applied flexibly whenever adaption is triggered in the verification CTs, see Fig. 2 in Appendix B for the workflow. For verification purposes, the plan can be recalculated using the verification CT to confirm if the plan satisfies the dosimetric

[1] https://cmiclab.cs.ucl.ac.uk/mmodat/niftyreg.

Table 1
Dosimetric goals of the treatment plans created in this study.

Structure	Goal under uncertainty	Priority
High-risk CTV	D_{95} (The minimum dose to 95 % of target volume) > 95 % of prescription dose (72.6 Gy(RBE), 33 fractions)	1
Low-risk CTV	D_{95} > 95 % of prescription dose (63 Gy(RBE), 33 fractions)	1
CTV	D_2 (The minimum dose to the hottest 2 % volume) < 107 % of prescription dose	1
Spinal cord	D_{max} (The maximum dose in the volume) < 45 Gy(RBE)	2
Brainstem	D_{max} < 55 Gy(RBE)	2
Chiasm	D_{max} < 55 Gy(RBE)	2
Structure	Goal in nominal	
Parotid glands	D_{mean} (The mean dose in the volume) < 26 Gy(RBE)	3
Oral Cavity	D_{mean} < 40 Gy(RBE)	3
Larynx	D_{mean} < 40 Gy(RBE)	3

goals. QA can be done immediately after the confirmation or even before it is needed, saving time of planning and calculation.

For comparison, the standard adaption plan was optimised on the verification CT which triggered the replan and applied to the treatment of the following week, representing a delay of 5 fractions before implementing the replan. An illustration of workflow difference between predicted plan adaption and standard replan is shown in Fig. 3 in Appendix B.

Because plan adaption was triggered with the aim of protecting the parotid glands, the overlap of the predicted contours (used in the predicted plan adaption strategy) and the real contours (used in the standard replan technique) for the parotid glands were measured by the Dice similarity coefficient(DSC) and compared with no model, where the contours in the planning CT replaced the predicted contours.

Although we applied our predicted replan flexibly in our strategy, the predicted replan week can be compared with the actual replan week to evaluate the predictive ability of our method.

2. Plan evaluation using accumulated dose metrics.

For both the predicted plan adaption and standard replan technique, we calculated the dose on the weekly verification CTs and deformed them to the planning CT to accumulate the dose, allowing an evaluation of the delivered dose to the patient. The accumulated dose using the standard replan technique is taken as the gold standard. The dose metrics of the plans (nominal plan, standard and predicted plan adaption) that are used for plan comparison are the same as in Table 1. The dosimetric details of all plans generated for this study are summarised in Table A2 in Appendix A.

Equation 1 is used to calculate the dose metrics difference between accumulated dose and planned dose.

$$\Delta Dx = Dx_{accu} - (Dx_n * F_n + Dx_r * F_r) \quad (1)$$

Dx represents a dose metric, ΔDx is the dose metric difference between accumulated dose and planned dose. Dx_{accu} is the dose metric of accumulated dose. Dx_n is the dose metric of the nominal plan. F_n is the number of fractions to which the nominal plan is applied. Dx_r is the dose metric of the adaptive replan, and F_r is the number of fractions to which the replan is applied. The planned dose is represented by the sum $Dx_n * F_n + Dx_r * F_r$.

A two-sample t-test (with a significance level of $p < 0.05$) was used to determine if there is a significant difference between the distribution of ΔDx in the two adaption strategies.

Results

The predictive power of the method is shown in Fig. 1 including DSC and replan week comparison. The DSC of the parotid glands (DSC_{PG}) between predicted contours (used in the predicted plan adaption) and the real contours (used in the standard replan) are compared with no model, in which planning contours and real contours in the standard replan are compared, in Fig. 1a. Using the predictive model, DSC_{PG} was increased by 0.08.

Deviation of the actual replan week from the predicted replan week is shown in Fig. 1b. Of note, we did not apply the predicted plan to the predicted week but applied it flexibly on the actual week that requires replan. In 4/10 cases, the predicted images accurately predicted the replan week (one patient that didn't need a replan is included in this scenario). In the remaining 6/10 cases, the predicted week and actual replan week differed by only 1 week.

Table 2 shows the nominal plan and the accumulated doses with no adaption, the standard replan and the predicted plan adaption for each patient except patient 1. For patient 1, unlike patients 2–10, the dose recalculation on the weekly verification CTs and predicted CTs did not trigger a replan and therefore no plans were generated for the standard replan and the predicted plan adaption.

In Fig. 2a, we compare the predicted plan adaption strategy with the standard replan technique and no adaption for all 10 patients in terms of dose metric differences ΔDx. We observed small mean and median differences of D_{95} between accumulated dose and planned dose for the CTVs, with a mean difference observed to the high-risk CTV of −1.20 %, −1.23 % and −1.25 % for no adaption, standard and predicted adaption, respectively. For the parotid glands, we find that for both adaption strategies the accumulated dose is within 3 Gy(RBE) of the planned dose; 2.34 Gy(RBE) and 2.03 Gy(RBE) for standard and predicted adaption, respectively, compared with 3.91 Gy(RBE) for no adaption. Furthermore, the mean dose of the parotid glands using the predicted plan adaption strategy is generally lower than using a standard replan, with 0.31 Gy(RBE) on average. Of note, the parotid glands D_{mean} in the predicted plan adaption is observed to be lower than that for the standard replan in some cases (for example, patient 3 in Appendix A) because they are optimized on a different geometry (predicted replans use predicted CTs while standard replans use verification CTs). In Fig. 2a that bias is removed using the difference in the dose metrics. If we apply the standard replan starting on the same day as the predicted adaption, the benefit of no delay in treatment using the standard replan is on average 0.47 Gy(RBE) to the parotid ΔD_{mean} (0.09 Gy(RBE) per fraction). The standard replan approach benefits from an additional 0.16 Gy(RBE) of sparing compared to the predicted adaption. However, any improvement in sparing is only realised when the replan is started on the same or next day. Fig. 2b–2c shows that all accumulated dose metrics of CTVs and serial OARs satisfy the clinical goals set for the plans.

Statistical analysis using a two-sample t-test demonstrates that the accumulated dose difference between no adaption and standard replan is only statistically significant ($p < 0.05$) in the parotid

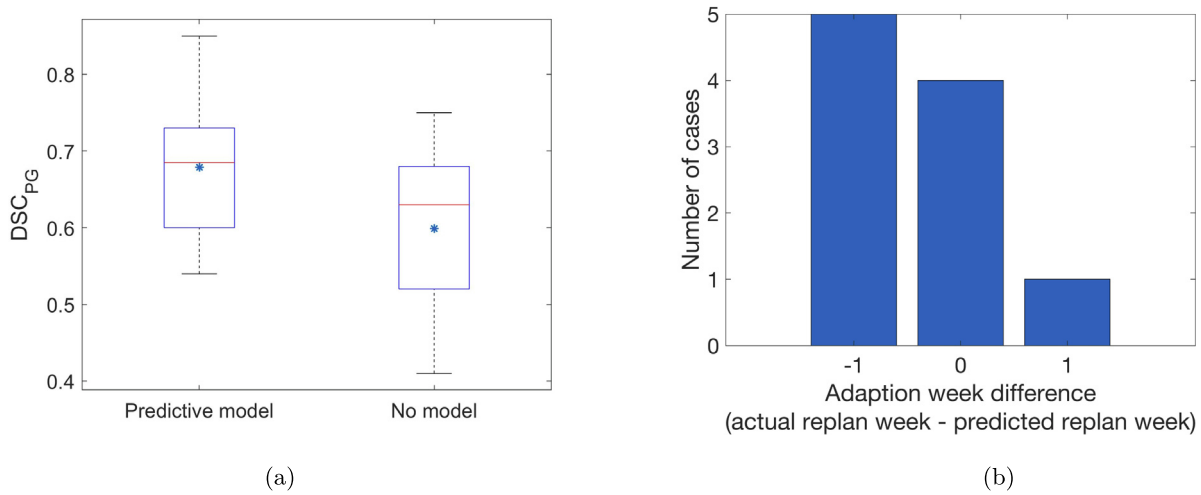

Fig. 1. (a) The comparison between the predictive model and no model on DSC_{PG} for the ten validation patients. The horizontal lines in the box plot indicate the median value among 10 patients, and the asterisks indicate the mean value. (b) Deviation of the actual replan week from the predicted replan week.

Table 2
Nominal and accumulated dose metrics of patients. Please note that for patient 1, no replan was triggered according to our criteria. The dose metrics for the parotid glands are highlighted in bold. The asterisk in the plan column indicates the numbers in the same row are the accumulated dose.

ID	Plan	High-risk CTV D_{95} (%)	Low-risk CTV D_{95} (%)	D_2 (%)	Spinal cord D_{max} Gy(RBE)	Brainstem D_{max} Gy(RBE)	Chiasm D_{max} Gy(RBE)	Parotid glands D_{mean} Gy(RBE)	Oral Cavity D_{mean} Gy(RBE)	Larynx D_{mean} Gy(RBE)
1	Nominal plan	98.75	98.86	103.05	30.55	45.69	36.5	27.36	6.8	30.93
	No Adaption*	97.93	98.89	103.17	28.56	42.39	27.5	29.61	6.9	31.14
2	Nominal plan	98.28	98.66	102.92	34.49	40.08	22.06	25.53	14.24	26.24
	No Adaption*	96.6	95.71	102.89	33.39	40.63	22.16	31.87	17.45	32.03
	Standard Replan*	97.11	96.67	101.79	35.45	40.54	20.64	**29.59**	16.24	26.89
	Predicted plan adaption*	96.6	96.35	102.62	35.81	41.27	19.45	**28.92**	17.39	28.43
3	Nominal plan	98.75	98.59	102.24	33.13	39.16	23.88	22.89	10.88	11.77
	No Adaption*	97.97	98.89	102.07	30.59	35.69	24.58	24.53	10.76	12.36
	Standard Replan*	98.05	98.89	101.52	30.28	35.55	23.53	**23.65**	11.19	12.16
	Predicted plan adaption*	98.05	98.89	102.07	31.34	38.28	23.8	**22.77**	10.48	11.27
4	Nominal plan	98.42	98.82	102.96	32.9	34.4	32.02	24.53	7.43	22.18
	No Adaption*	97.74	97.94	102.62	30.47	29.68	29.29	28.36	8.62	25.09
	Standard Replan*	97.86	97.62	101.79	23.85	32.26	27.3	**26.05**	8.11	20.84
	Predicted plan adaption*	97.82	96.98	102.07	24.36	33.89	22.04	**25.03**	8.31	21.39
5	Nominal plan	98.82	98.67	102.02	34.56	40.75	26.21	23.63	10.65	16.08
	No Adaption*	98.09	98.57	102.34	39.36	42.39	28.91	28.61	12.19	19.99
	Standard Replan*	97.97	98.89	101.79	37.18	42.65	26.98	**26.08**	11.88	18.57
	Predicted plan adaption*	98.01	98.57	102.07	35.86	42.18	28.89	**24.66**	12.24	19.5
6	Nominal plan	98.5	98.65	102.7	36	38.93	34.37	29.65	15.38	30
	No Adaption*	97.38	98.57	102.89	39.86	41.68	32.99	32.95	17.14	28.37
	Standard Replan*	97.03	98.25	101.79	37.74	41.93	32.98	**30.44**	16.15	27.41
	Predicted plan adaption*	96.79	97.94	102.34	38.81	43.56	31.84	**31.3**	16.29	28.04
7	Nominal plan	98.6	98.27	102.58	36.53	40	26.86	27.04	13.19	19.64
	No Adaption*	97.03	98.57	102.34	36.77	39.05	28.31	30	12.98	23.13
	Standard Replan*	96.64	98.25	102.34	34.33	38.22	26.29	**28.87**	12.61	21.04
	Predicted plan adaption*	96.91	98.25	102.07	36.41	39.67	28.45	**28.07**	12.33	21.05
8	Nominal plan	98.37	98.63	102.48	35.47	36.01	23.43	27.24	10.6	19.77
	No Adaption*	96.44	97.62	102.34	32.27	30.41	23.88	29.25	11.86	20.77
	Standard Replan*	96.6	97.94	102.07	33.2	31.9	22.67	**28.66**	11.78	19.51
	Predicted plan adaption*	96.6	97.94	102.34	29.13	31.14	23.99	**28.48**	11.98	20.91
9	Nominal plan	98.75	98.76	102.31	11.84	42.58	42.63	22.66	8.83	9.2
	No Adaption*	96.95	98.25	102.62	14.78	52.68	41.76	27.14	9.45	17.64
	Standard Replan*	96.95	98.25	102.07	15.2	47.39	38.97	**25.2**	10.14	14.67
	Predicted plan adaption*	96.75	98.57	102.07	12.14	49.15	40.14	**24.86**	9.2	13.68
10	Nominal plan	98.62	98.28	102.01	29.2	38.76	36.3	27.64	7.1	21.44
	No Adaption*	97.7	97.62	102.07	32.28	36.51	37.21	31.47	7.21	21.9
	Standard Replan*	97.54	96.98	101.24	33.62	39.52	37.66	**30.29**	7.06	20.12
	Predicted plan adaption*	97.78	97.3	101.79	32.92	35.07	38.78	**30**	7.86	21.07

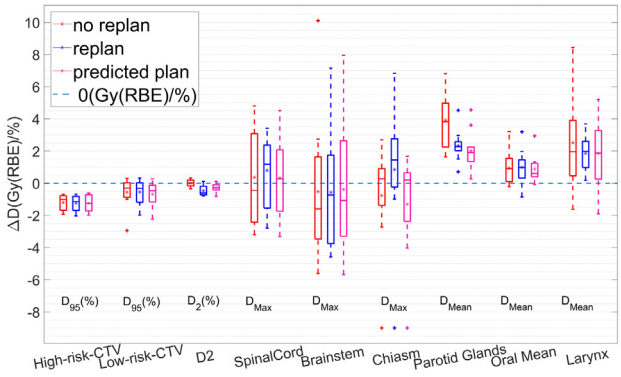

(a) Dose metric differences between accumulated dose and planned dose (see equation 1) of three adaption strategies.

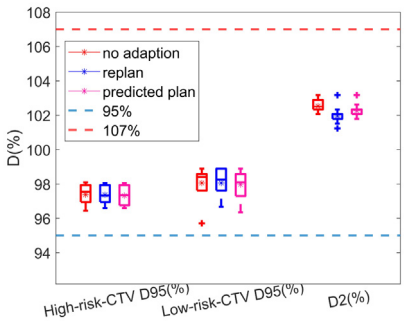

(b) Accumulated D_{95} and D_2 for the high-risk and low-risk CTV.

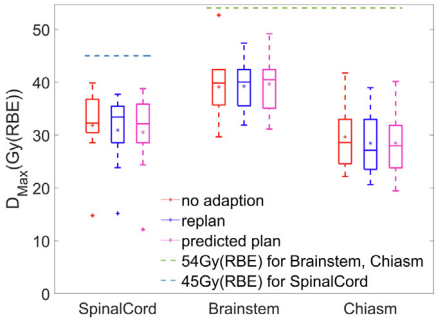

(c) Accumulated D_{max} for the serial organs

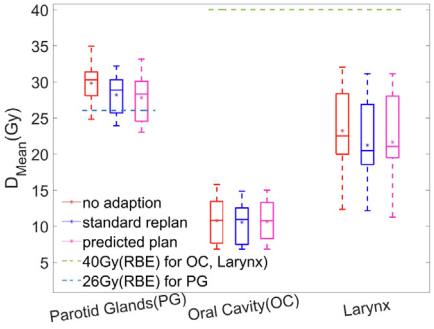

(d) Accumulated D_{mean} for the parallel organs

Fig. 2. Comparison of the dose metric differences and accumulated dose metrics for 10 patients observed in no adaption, standard replan and predicted plan adaption. The horizontal lines in the box plot indicate the median. dose metric difference among 10 patients, and the asterisks indicate the mean difference. (a) shows the dose metric differences. D_{max} and D_{mean} are given in units of Gy(RBE). (b)–(c) shows the accumulated dose metrics. The dashed lines in (b)–(d) represent the defined clinical goals summarised in Table 1.

gland D_{mean} and $D_{2\%}$. The difference between standard replan and predicted plan adaption was not found to be significant (see Table 3).

The weekly changes in dose metrics for the CTVs and parotid glands are shown in Fig. 3 for each patient. There are scenarios in which using the initial tumour contour from the planning CT in the predicted plan show a better coverage than using the real tumour contour, for example, patient 9 at week 5 in Fig. 3a, because larger contours can mitigate the variation during the treatment. In the TORPEdo trial, therapeutic target volumes are not adapted according to changes in GTV. However, some patients presented with a displacement of the tumour that extended outside the original contour[20], such as patient 2 at week 5 in Fig. 3a. In such cases, the predicted replan using the initial contour is inferior to the standard replan. An alternative approach would be to use the contours from the latest weekly repeat CT for predicted plan adaption.

In Fig. 3f, we observe that for most patients, plan adaptions occur around the 3rd (6/10) or 4th (2/10) week of treatment, which is consistent with the conclusion of Brown *et al.* [25] and Wu *et al.* [26].

Discussion

The offline adaptive strategy used in radiotherapy clinics can cause gaps in treatments or the delivery of suboptimal fractions due to delays in implementation of an adapted plan and can challenge clinical workflow efficiency. We exploited a predictive anatomical model to prepare adaptive plans in advance. Our results show that a predicted plan adaption strategy using the predictive anatomical model can achieve similar CTV coverage and reduce parotid dose compared to the standard replanning approach.

In this work, the benefit of a no-delay treatment on parotid glands D_{mean} is 0.31 Gy(RBE) on average. For patient 6, the predicted anatomy which was used to create a prospective replan suggested the need for adaption due to a change in the mean parotid dose of > 3 Gy(RBE). However, while a parotid ΔD_{mean} in the nominal plan on the predicted anatomy was 3.05 Gy(RBE), the parotid ΔD_{mean} calculated on the triggering verification CT of week 3 was 6.35 Gy(RBE). A dramatic shrinkage of the volume between week 2 and week 3 made the predicted model less effective in this case. Despite this, when we applied the predicted plan on week 3, the parotid ΔD_{mean} on the verification CT of week 3 was reduced to 3.05 Gy(RBE). In this circumstance, we might look to apply the predicted replan on week 3 and follow the standard replan procedure to create a new replan. This limitation can potentially be improved if patients are stratified by exploiting tumour related features [27,28] and outlining change-related features [29–31] based on a larger dataset. Another scenario worth discussing is where the dose recalculation on the predicted images indicated a parotid ΔD_{mean} that did not reach the triggering threshold but was close

Table 3
p-Value of the two-sample t-test between the distribution of ΔDx (see equation 1) in two adaption strategies with mean value(μ) and standard deviation(σ). The capitals in parenthesis indicate no adaption(N), standard replan(S), and predicted plan adaption(P). Statistically significant differences between plans (taken as $p < 0.05$) are highlighted in bold.

Statistics	High-risk CTV D_{95} (%)	Low-risk CTV D_{95} (%)	D_2 (%)	Spinal cord D_{max} Gy(RBE)	Brainstem D_{max} Gy(RBE)	Chiasm D_{max} Gy(RBE)	Parotid D_{mean} Gy(RBE)	Oral Cavity D_{mean} Gy(RBE)	Larynx D_{mean} Gy(RBE)
No Adaption ($\mu\pm\sigma$)	−1.203 ± 0.491	−0.556 ± 0.96	0.007 ± 0.23	0.365 ± 3.029	−0.525 ± 4.623	−0.767 ± 3.267	3.913 ± 1.773	0.945 ± 1.071	2.516 ± 3.009
Standard replan ($\mu\pm\sigma$)	−1.236 ± 0.495	−0.545 ± 0.753	−0.466 ± 0.325	0.795 ± 2.181	−0.571 ± 3.715	0.848 ± 4.073	2.337 ± 0.989	0.989 ± 1.125	1.855 ± 1.248
Flexible plan adaption ($\mu\pm\sigma$)	−1.252 ± 0.567	−0.685 ± 0.823	−0.295 ± 0.271	0.328 ± 2.307	−0.383 ± 4.036	−1.301 ± 3.201	2.03 ± 1.265	0.87 ± 0.867	1.846 ± 2.206
p value (N and S)	0.883	0.978	**0.001**	0.72	0.981	0.341	**0.024**	0.929	0.529
p value (S and P)	0.947	0.697	0.216	0.647	0.915	0.206	0.553	0.794	0.991

to it, for example, 2.75 Gy(RBE). In this case, we would suggest having an alternative plan available in case re-planning would be triggered.

We only considered 1-step adaption for the proof of concept. In Fig. 3e), the parotid mean dose difference of some patients in week 4 is still more than 3 Gy(RBE), because of severe shrinkage. For example, patient 2 adapted the plan on week 3 with parotid D_{mean} of 25 Gy(RBE), however, when the adapted plan was applied to week 4 the parotid D_{mean} increased to 32 Gy(RBE). In this case, a second adaption is needed. If we update the model every time that a new CT is acquired then the prediction for a second adaption is clearly possible.

In clinical practice, plans are robustly optimised to account for setup and range uncertainties and, while anatomical changes may not be included explicitly in the optimisation process, it is possible that some robustness to anatomical changes is provided by an improved robustness to these setup and range uncertainties. Where the magnitude of setup errors in the robust optimisation is reduced, plans would likely be more sensitive to anatomical changes. As such, the application of predictive anatomical modelling to the design of a robust plan may allow for a reduced setup robustness margin, thereby improving dose conformity to some extent. Though there may be a trade-off between this margin and the number of plan adaptations required during a treatment course. Furthermore, there use of a predictive model as an additional error scenario in the robust optimisation may be of interest though further work is required to understand the detriment to the nominal plan of such robustness. The predictive nature of our approach can enable improved workflow management. It also should be noted that robust beam angle selection remains critical for avoiding anatomical variations such as nasal filling. Such variations cannot be modelled by deformations.

For this proof of concept, images from a cohort of 20 patients were used. This cohort was particularly suited to this study, having weekly CTs with manually delineated contours. In contrast, the use of weekly cone-beam CTs (CBCT), which are more commonly available, are subject to additional DIR uncertainty. Secondly, the error from HU correction required by CBCT is removed. We can directly calculate the dose distribution and create a replan. In addition, we can directly calculate the weekly dose metrics using the manually delineated contours on weekly CTs. Further validation of the model will be conducted on a larger cohort of patients. We are currently working on finding the optimal parameters for patients who have received IMPT with CBCT data but the procedure of using CBCT images to build the model is the same. For patients treated with IMPT, because their progressive anatomical changes may be smaller than of those undergoing photon therapy [2,32], the uncertainty of DIR used to build the model can be reduced [33–35] resulting in an improved model accuracy. Thus, methods presented here are easily transferable to a patient dataset having received proton therapy. The feasibility of using the model to apply predicted plans on a fixed week to reduce the number of validation CTs has been demonstrated in Appendix C. Accurately predicting the week in which plan adaption is required and further evaluation on other organs are important next steps in implementing prospective offline adaptive therapy.

In the literature, anatomical models have only been used for DIR evaluation [36] or assessed based on the misalignment of the anatomical landmarks [37,38]. In this paper, we evaluated an anatomical model based on the dose distribution. This is the first demonstration of the potential of the anatomical model in adaptive radiotherapy. Compared to online adaption [13–15], our method can reduce the treatment time by preparing complete adaptive plans in advance without further optimisation and the need for real-time QA, which is one of the most challenging aspects of online adaption. Furthermore, by exploiting novel auto-planning

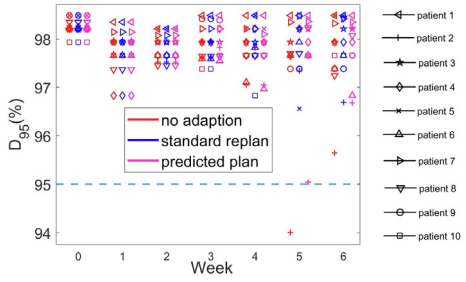

(a) Weekly D_{95} of high-risk CTV for each patient.

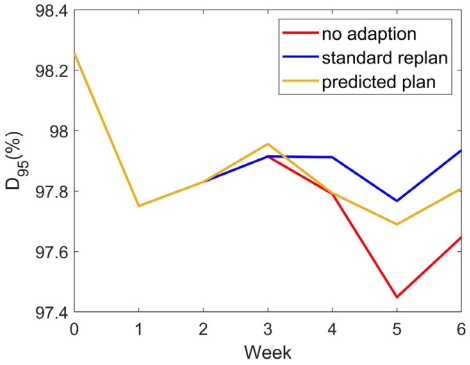

(b) Average D_{95} of high-risk CTV for each week.

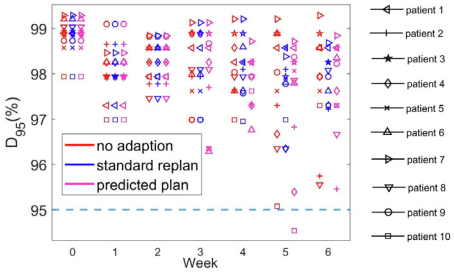

(c) Weekly D_{95} of low-risk CTV for each patient.

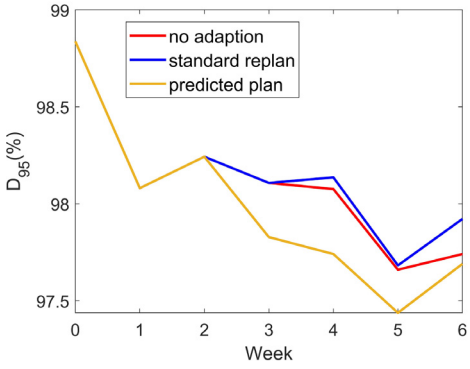

(d) Average D_{95} of low-risk CTV for each week.

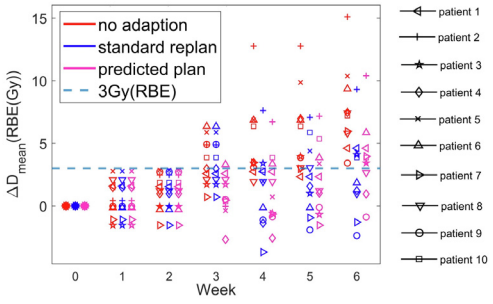

(e) Difference D_{mean} (between weekly D_{mean} and D_{mean} of week 0 (planning CT)) of parotid glands for each patient.

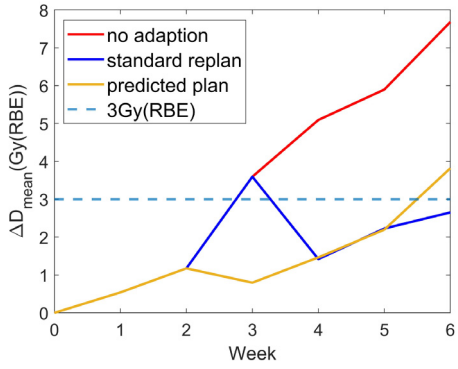

(f) Average difference D_{mean} (between weekly D_{mean} and D_{mean} of week 0 (planning CT)) of parotid glands for each week.

Fig. 3. The weekly dose metrics for 10 patients observed in no adaption, standard replan, and predicted plan adaption. Patients are represented using different markers. b), d), and f) are the average results over 10 patients.

techniques [39], our method may allow for auto-replanning for adaptive IMPT.

Conclusion

Prediction based prospective replanning could potentially enable clinically acceptable adaptive therapy without treatment gaps or sub-optimal fractions to be delivered due to delays in standard adaptive strategies, leading to an improved overall treatment course for patients. Furthermore, the ability to manage the adaptive therapy workflow prospectively with a predictive approach can increase the efficiency of a busy clinical proton therapy centre.

Funding statement

Ying Zhang is supported by a scholarships from the China Scholarship Council Nos. 201809150003. Esther Bär is supported by the Radiation Research Unit at the Cancer Research UK City of London. Centre Award C7893/A28990. Richard Amos is supported by a Cancer Research UK Centres Network Accelerator.

Award Grant (A21993) to the ART-NET Consortium. Wenyong Tan is supported by the National Natural Science. Funding of China (81974462).

Data share statement

Restricted access. The authors cannot make these data publicly available due to data use agreement.

Declaration of Competing Interest

The authors declare that they have no known competing financial interests or personal relationships that could have appeared to influence the work reported in this paper.

Appendix A. Supplementary data

Supplementary data to this article can be found online at https://doi.org/10.1016/j.radonc.2022.05.036.

References

[1] Steneker M, Lomax A, Schneider U. Intensity modulated photon and proton therapy for the treatment of head and neck tumors. Radiother Oncol 2006;80:263–7.
[2] Van De Water TA, Lomax AJ, Bijl HP, De Jong ME, Schilstra C, Hug EB, et al. Potential benefits of scanned intensity-modulated proton therapy versus advanced photon therapy with regard to sparing of the salivary glands in oropharyngeal cancer. Internat J Radiat Oncol Biol Phys 2011;79:1216–24.
[3] McGowan SE, Burnet NG, Lomax AJ. Treatment planning optimisation in proton therapy. Brit J Radiol 2013;86.
[4] Minatogawa H, Yasuda K, Dekura Y, Takao S, Matsuura T, Yoshimura T, et al. Potential benefits of adaptive intensity-modulated proton therapy in nasopharyngeal carcinomas. J Appl Clin Med Phys 2021;22:174–83.
[5] Lester-Coll NH, Margalit DN. Modeling the potential benefits of proton therapy for patients with oropharyngeal head and neck cancer. Internat J Radiat Oncol Biol Phys 2019;104:563–6.
[6] Brouwer CL, Steenbakkers RJHM, Langendijk JA, Sijtsema NM. Identifying patients who may benefit from adaptive radiotherapy: Does the literature on anatomic and dosimetric changes in head and neck organs at risk during radiotherapy provide information to help. Radiother Oncol 2015;115:285–94.
[7] Cheng HCY, Wu VWC, Ngan RKC, Tang KW, Chan CCL, Wong KH, et al. A prospective study on volumetric and dosimetric changes during intensity-modulated radiotherapy for nasopharyngeal carcinoma patients. Radiother Oncol 2012;104:317–23.
[8] Wu RY, Liu AY, Sio TT, Blanchard P, Wages C, Amin MV, et al. Intensity-modulated proton therapy adaptive planning for patients with oropharyngeal cancer. Internat J Particle Therapy 2017;4:26–34.
[9] Zhiyong Yang, Xiaodong Zhang, Xianliang Wang, X. Ronald Zhu, Brandon Gunn, Steven J. Frank, Yu Chang, Qin Li, Kunyu Yang, Gang Wu, Li Liao, Yupeng Li, Mei Chen, and Heng Li. Multiple-CT optimization: An adaptive optimization method to account for anatomical changes in intensity-modulated proton therapy for head and neck cancers. *Radiotherapy and Oncology*, 142:124–132, 2020.
[10] Yang H, Hu W, Wang W, Chen P, Ding W, Luo W. Replanning during intensity modulated radiation therapy improved quality of life in patients with nasopharyngeal carcinoma. Internat J Radiat Oncol Biol Phys 2013;85:e47–54.
[11] Zhao L, Wan Q, Zhou Y, Deng X, Xie C, Shixiu Wu. The role of replanning in fractionated intensity modulated radiotherapy for nasopharyngeal carcinoma. Radiother Oncol 2011;98:23–7.
[12] Suzuki K, Gillin MT, Narayan Sahoo X, Zhu R, Lee AK, Lippy D. Quantitative analysis of beam delivery parameters and treatment process time for proton beam therapy. Med Phys 2011;38:4329–37.
[13] Botas P, Kim J, Winey B, Paganetti H. Online adaption approaches for intensity modulated proton therapy for head and neck patients based on cone beam CTs and Monte Carlo simulations. Phys Med Biol 2018;64:015004.
[14] Bobić M, Lalonde A, Sharp GC, Grassberger C, Verburg JM, Winey BA, et al. Comparison of weekly and daily online adaptation for head and neck intensity-modulated proton therapy. Phys Med Biol 2021;66:055023.
[15] Lalonde Arthur, Mislav Bobíc, Winey Brian, Verburg Joost, Sharp Gregory C, Paganetti Harald. Anatomic changes in head and neck intensity-modulated proton therapy: comparison between robust optimization and online adaptation. Radiother Oncol 2021;159:39–47.
[16] BFCO. Timely delivery of radical radiotherapy: guidelines for the management of unscheduled treatment interruptions. fourth ed. The Royal College of Radiologists; 2019.
[17] Zhang Y, McGowan Holloway S, Zoë Wilson M, Alshaikhi J, Tan W, Royle G, et al. DIR-based models to predict weekly anatomical changes in head and neck cancer proton therapy. Phys Med Biol 2022;67:095001.
[18] Price J, Hall E, West C, Thomson D. TORPEdO-A phase III trial of intensity-modulated proton beam therapy versus intensity-modulated radiotherapy for multi-toxicity reduction in oropharyngeal cancer. Clin Oncol (Royal College of Radiologists (Great Britain)) 2020;32:84–8.
[19] Brouwer CL, Steenbakkers RJHM, van der Schaaf A, Sopacua CTC, van Dijk LV, Kierkels RGJ, et al. Selection of head and neck cancer patients for adaptive radiotherapy to decrease xerostomia. Radiother Oncol 2016;120:36–40.
[20] Tan Wenyong, Li Yanping, Han Guang. Target volume and position variations during intensity-modulated radiotherapy for patients with nasopharyngeal carcinoma. OncoTargets Therapy 2013;6:1719.
[21] Lee AW, Ng WT, Pan JJ, Chiang C-L, Poh SS, Choi HC, et al. International guideline on dose prioritization and acceptance criteria in radiation therapy planning for nasopharyngeal carcinoma. Internat J Radiat Oncol Biol Phys 2019;105:567–80.
[22] Lewis GD, Holliday EB, Kocak-Uzel E, Hernandez M, Garden AS, Rosenthal DI, et al. Intensity-modulated proton therapy for nasopharyngeal carcinoma: Decreased radiation dose to normal structures and encouraging clinical outcomes. Head Neck 2016;38:E1886–95.
[23] Evans JD, Harper RH, Petersen M, Harmsen WS, Anand A, Hunzeker A, et al. The importance of verification CT-QA scans in patients treated with IMPT for head and neck cancers. Internat J Particle Therapy 2020;7:41–53.
[24] Veiga C, Lourenço AM, Mouinuddin S, van Herk M, Modat M, Ourselin S, et al. Toward adaptive radiotherapy for head and neck patients: Uncertainties in dose warping due to the choice of deformable registration algorithm: Dose warping uncertainties due to registration algorithm. Med Phys 2015;42:760–9.
[25] Brown E, Owen R, Harden F, Mengersen K, Oestreich K, Houghton W, et al. Head and neck adaptive radiotherapy: Predicting the time to replan. Asia-Pacific J Clin Oncol 2016;12:460–7.
[26] Wu Q, Nandalur SR, Nandalur KR, Krauss DJ, Chen PY, Yan D, et al. What time is optimal for replanning head and neck IMRT (HN-IMRT)? Internat J Radiat Oncol Biol Phys 2008;72:S163.
[27] Bogowicz M, Tanadini-Lang S, Guckenberger M, Riesterer O. Combined CT radiomics of primary tumor and metastatic lymph nodes improves prediction of loco-regional control in head and neck cancer. Sci Rep 2019;9:1–7.
[28] Lassen P, Eriksen JG, Hamilton-Dutoit S, Tramm T, Alsner J, Overgaard J. Effect of HPV-associated p16INK4A expression on response to radiotherapy and survival in squamous cell carcinoma of the head and neck. J Clin Oncol 2009;27:1992–8.
[29] van Dijk LV, Brouwer CL, van der Schaaf A, Burgerhof JGM, Beukinga RJ, Langendijk JA, et al. CT image biomarkers to improve patient-specific prediction of radiation-induced xerostomia and sticky saliva. Radiother Oncol 2017;122:185–91.
[30] Gabryś HS, Buettner F, Sterzing F, Hauswald H, Bangert M. Design and selection of machine learning methods using radiomics and dosiomics for normal tissue complication probability modeling of xerostomia. Front Oncol 2018;8.
[31] Brivio Davide, Yida David Hu, Margalit Danielle N, Zygmanski Piotr. Selection of head and neck cancer patients for adaptive replanning of radiation treatment using kV-CBCT. Biomed Phys Eng Express 2018;4.
[32] Sio TT, Lin H-K, Shi Q, et al. Intensity modulated proton therapy versus intensity modulated photon radiation therapy for oropharyngeal cancer: first comparative results of patient-reported outcomes. Internat J Radiat Oncol Biol Phys 2016;95:1107–14.
[33] Zhong H, Chetty IJ. Caution must be exercised when performing deformable dose accumulation for tumors undergoing mass changes during fractionated radiation therapy. Internat J Radiat Oncol Biol Phys 2017;97:182–3.
[34] Nenoff L, Ribeiro CO, Matter M, Hafner L, Josipovic M, Langendijk JA, et al. Deformable image registration uncertainty for inter-fractional dose

accumulation of lung cancer proton therapy. Radiother Oncol 2020;147:178–85.
[35] Veiga C, Janssens G, Teng C-L, Baudier T, Hotoiu L, McClelland JR, et al. First clinical investigation of cone beam computed tomography and deformable registration for adaptive proton therapy for lung cancer. Internat J Radiat Oncol Biol Phys 2016;95:549–59.
[36] Yu ZH, Kudchadker R, Dong L, Zhang Y, Court LE, Mourtada F, et al. Learning anatomy changes from patient populations to create artificial CT images for voxel-level validation of deformable image registration. J Appl Clin Med Phys 2016;17:246–58.
[37] Chetvertkov MA, Siddiqui F, Chetty I, Kim J, Kumarasiri A, Liu C, et al. Use of regularized principal component analysis to model anatomical changes during head and neck radiation therapy for treatment adaptation and response assessment. Med Phys 2016;43:5307–19.
[38] Van Kranen Simon, Mencarelli Angelo, Beek Coen Rasch Suzanne Van, Van Herk Marcel, Sonke Jan Jakob. Adaptive radiotherapy with an average anatomy model: Evaluation and quantification of residual deformations in head and neck cancer patients. Radiother Oncol 2013;109:463–8.
[39] Kouwenberg J, Penninkhof J, Habraken S, Zindler J, Hoogeman M, Heijmena B. Model based patient pre-selection for intensity-modulated proton therapy (IMPT) using automated treatment planning and machine learning. Radiother Oncol 2021;6:224–9.